

# A Novel $\text{Co}_3\text{O}_4\text{-BiPO}_4$ Nanoarchitectonics Material Preparation for the Electrocatalytic Detection of Epinephrine

麻醉部 陸翔寧

Hsiang-Ning Luk<sup>1</sup>, Yi-Hsin Chen<sup>2</sup>, Chia-Ying Hsieh<sup>2</sup>, Yan Wei Han<sup>2</sup>, Ren-Jang Wu<sup>2,\*</sup>, and Murthy Chavali<sup>3,4,\*</sup>

<sup>1</sup>Department of Anesthesia, Hualien Tzu-Chi Hospital, Hualien 97002, Taiwan, ROC

<sup>2</sup>Department of Applied Chemistry, Providence University, Shalu, Taichung 43301, Taiwan, ROC

<sup>3</sup>Shree Velagapudi Ramakrishna Memorial College, Nagaram 522268, Guntur Dt., AP, India

<sup>4</sup>Mc Education, Training, Research and Consultancy, Tenali, Guntur 522201, Andhra Pradesh, India

A novel sensing material of cobalt oxide-bismuth phosphate ( $\text{Co}_3\text{O}_4\text{-BiPO}_4$ ) was prepared by the hydrothermal method. Thus prepared sensing material was characterized by X-ray diffraction analysis (XRD) and transmission electron microscopy (TEM). The sensor was used for the determination of epinephrine by using modified  $\text{Co}_3\text{O}_4\text{-BiPO}_4$  on glassy carbon electrode (GCE). The cyclic voltammetry (CV) and differential pulse voltammetry (DPV) methods showed a wide linear response to a concentration range, from 1.71 to 55.00  $\mu\text{M}$ , and the epinephrine detection limit for this sensing system was found to be 1.334  $\mu\text{M}$ . The  $\text{Co}_3\text{O}_4\text{-BiPO}_4$  electrode has very high selectivity towards the detection of epinephrine supported by an interference test. The epinephrine sensor seems very advantageous for future clinical health and medical sectors.

**Keywords:** Epinephrine, Cyclic Voltammetry, Differential Pulse Voltammetry (DPV),  $\text{Co}_3\text{O}_4\text{-BiPO}_4$ .

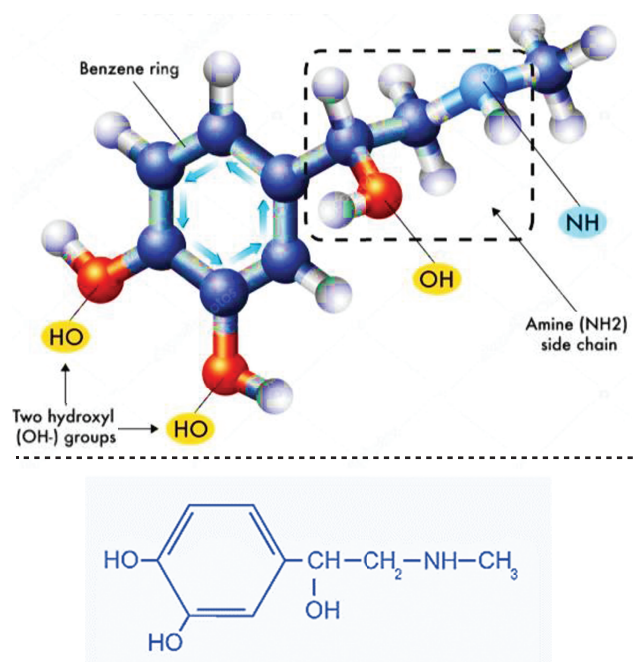
## 1. INTRODUCTION

Epinephrine (EP) is a neurotransmitter (catecholamine family) essential for human body functions. It is produced under stress in adrenal glands and is necessary for the sympathetic nervous functions. The chemical structure of epinephrine (Adrenaline) along with the chemical identifiers is illustrated in Figure 1. Generally, EP is indicated for patients with cardiac arrest, anaphylaxis, asthma and also used as a vasoconstrictor (e.g., combined use with local anaesthetics). The dosage of intravenous EP as a positive inotrope is ranged from 0.01 to 1 microgram/kg/min. In contrast, an initial dose of 100–300 microgram EP intravenously has been recommended for treating anaphylaxis. Side effects of EP include palpitation, tachycardia, cardiac arrhythmia, anxiety, headache, tremble, hypertension and pulmonary oedema. An excessive amount of epinephrine causes the rising of the patient's blood pressure, sudden numbness, garbled dialogue and worsened breathing.

A potential health crisis may occur due to epinephrine overdose. Several illnesses, such as Cushing's and Conn's syndromes, are related to the changes in plasma epinephrine concentration. Thus, it is obliged to develop new low-cost, simple, and accurate quantitative methods to diagnose related diseases and to measure the concentrations of EP in the intravenous solution preparations for clinical practice [1, 2].

Up to now, epinephrine concentrations were determined by various techniques; including high-performance liquid chromatography-mass spectrometer (HPLC-MS) [1], fluid fluorescence [2], capillary electrophoresis [3] and types of electrochemical analysis [4]. Although high-performance liquid chromatography-mass spectrometer, fluid fluorescence and capillary electrophoresis had very high accuracy, the cost of the instrument was high and it could not be measured in time. The development of an electrochemical method to detect epinephrine with low cost and rapid speed was necessary and required for setting up of easy online detection. Existing literature suggests,

\*Authors to whom correspondence should be addressed.

**IDENTIFIERS:**

IUPAC Name:	(R)-4-(1-Hydroxy-2-(methylamino)ethyl)benzene-1,2-diol
Formula:	$\text{C}_9\text{H}_{13}\text{NO}_3$
Synonyms:	Adrenaline (BAN UK)
CAS Number:	51-43-4
PubChem CID:	5816
IUPHAR/BPS:	479
DrugBank:	DB00668
ChemSpider:	5611
UNII:	YKH834O4BH
KEGG:	D00095
ChEBI:	CHEBI:28918
ChEMBL:	ChEMBL679
PDB ligand:	ALE (PDBe, RCSB PDB)
ECHA InfoCard:	100.000.090

**Figure 1.** Representation of 3D chemical structure of epinephrine (adrenaline) along with the chemical identifiers.

using a nanostructured Au electrode for the detection of epinephrine by linear sweep voltammetry (LSV) and differential pulse voltammetry (DPV) method. The LSV had shown good linearity with the epinephrine concentration range of 60–600  $\mu\text{M}$ . The DPV calibration curve for EP determination is linear in the range of 10–150  $\mu\text{M}$ , the detection limit of 2.8  $\mu\text{M}$  [5]. Researchers applied f-MWCNTs/BR9/GCE to determine serotonin and epinephrine simultaneously. The experimental methods of CV and DPV are a quantitative characterization of f-MWCNTs/BR9/GCE. The f-MWCNTs/BR9/GCE had high sensitivity, excellent stability for the detection limit of 9  $\mu\text{M}$  of EP [6]. SWCNT-CoTAPc electrode is performed to detect epinephrine with CV and EIS [7]. The CV is in EP concentration linear range 12.2–130  $\mu\text{M}$ , the sensitivity of  $9.4 \times 10^{-3} \text{ AM}^{-1}$  and a detection limit of 6  $\mu\text{M}$  [7].

In the past decade, there has been mounting attention in studying nanomaterials and their applications in solid-state electrochemical devices. Nanomaterials are a good choice for the alteration of electrodes due to their high surface area and good electrical conductivity. To overcome the limitation of the number of kinds of sensing material, a smart material as rod-like structure nanoarchitectonic is designed as this work; it is a technology allowing arrangement of nano-sized structural units [8, 9]. It can promote the sensor response of detection of the EP. The  $\text{Co}_3\text{O}_4$  is an important antiferromagnetic *p*-type semiconductor; a catalytic chemical oxidation reaction happens reversibly in two cobalt metal ions  $\text{Co}^{+2}$  and  $\text{Co}^{+3}$  metal oxides [10, 11]. It is easy to change the valence in the redox reaction.  $\text{Co}_3\text{O}_4$  is with exceptional properties such as gas-sensing, electrochemical and catalytic properties,

and has been investigated widely for applications in solid-state sensors, electrochromic devices and heterogeneous catalysts as well as lithium batteries [12].

$\text{BiPO}_4$  is a highly efficient photocatalyst, for oxidation reaction, and it can easily dope with other materials improving the catalytic properties [13]. In this study, owing to their excellent properties and expecting this system could be a better electrode material for the detection of epinephrine, we chose to combine  $\text{Co}_3\text{O}_4$  with  $\text{BiPO}_4$ , the prepared nanocomposite of  $\text{Co}_3\text{O}_4\text{-BiPO}_4$  has benefits of low cost, simple to make up on the electrode, excellent of electrocatalytic activity and promote electronic transfer and it seems to be a very promising sensing material used for electrochemical detection of epinephrine.

## 2. EXPERIMENTAL DETAILS

### 2.1. Materials

All the chemicals used in this study were of analytical reagent grade (AR) (Purity >99%) unless otherwise mentioned. Epinephrine (98%, Aladdin Industrial Corporation (Shanghai, China) and lidocaine were offered by Hualien Tzu-Chi Hospital (Buddhist Tzu Chi Medical Foundation, Chung Yang Rd., Hualien 970, Taiwan, ROC; <http://hlm.tzuchi.com.tw/en/>) and were used without any further purification.  $\text{Bi}(\text{NO}_3)_3 \cdot 5\text{H}_2\text{O}$ ,  $\text{Na}_3\text{PO}_4$ ,  $\text{CoCl}_2 \cdot 6\text{H}_2\text{O}$  were purchased from Alfa-Aesar and other chemicals  $\text{Na}_3\text{C}_6\text{H}_5\text{O}_7$  (SHOWA Chemicals),  $\text{NaOH}$  (UniRegion Bio-Tech)  $\text{HNO}_3$  (J. T. Backer) were procured. The supporting electrolyte was  $\text{NaCl}$  (0.9%, pH range 4.5–7.0). All the chemicals were used as received. Water was distilled

and de-ionized (DI) using a Milli-Q water purification system (Millipore Corp.).

## 2.2. Preparation of Sensing Materials

$\text{Co}_3\text{O}_4$  nanomaterials were obtained via the thermal treatment of cobalt oxalate nanorods synthesized through a convenient solvothermal route [14]. The process of preparation of Bismuth phosphate ( $\text{BiPO}_4$ ) nanorod is as follows. Bismuth phosphate was prepared for hydrothermal methods.  $\text{Bi}(\text{NO}_3)_3 \cdot 5\text{H}_2\text{O}$  and  $\text{Na}_3\text{PO}_4$  were blended as per their molar weight ratio of 2:1. With the addition of roughly around 45 mL D.I. water and 1 mL  $\text{HNO}_3$  while stirring continuously. The solution was placed in a Teflon container at 160 °C for 24 hours in the oven. Then the  $\text{BiPO}_4$  sample was washed with D.I. water and ethanol dried at 50 °C in a vacuum oven.  $\text{BiPO}_4$  was dispersed in 15 mL D.I. water. The  $\text{CoCl}_2 \cdot 6\text{H}_2\text{O}$  and  $\text{Na}_3\text{C}_6\text{H}_5\text{O}_7$  added to this solution while stirring continuously to which NaOH was added dropwise until the pH equals to 11, then the sample was prepared under hydrothermal conditions at 180 °C for 12 h. Later it was centrifuged and washed several times with D.I. water and ethanol dried in an oven at 80 °C. Moreover, the material  $\text{Co}_3\text{O}_4\text{-BiPO}_4$  was obtained by calcining at 300 °C for 2 h.

## 2.3. Preparation of $\text{Co}_3\text{O}_4\text{-BiPO}_4/\text{GCE}$

The reversibility of the electrode reaction at the carbon paste electrode is far superior to the glassy carbon electrode was understood. However, the carbon paste electrode is not suitable to use for the electrode reaction in a non-aqueous solution. Here, a simple preparation of the glassy carbon electrode, which can be used even in non-aqueous solution, was described. The working electrode was prepared as follows:

Prior to modification, the glassy carbon electrode (GCE, 3 mm dia.) was cleaned by polishing it with 0.01 mm  $\alpha\text{-Al}_2\text{O}_3$  powder and then carefully with a fine emery paper. Later using D.I. water, all the impurities on the GCE surface were washed off. The electrode surface was wiped with a filter paper. After washing with distilled water to remove  $\text{Al}_2\text{O}_3$  and other substances, the electrode surface was cleaned with ethanol carefully. Then the electrode was sonicated for about 5 min with distilled water and then acetone. An appropriate ratio of  $\text{Co}_3\text{O}_4\text{-BiPO}_4$  with 5% chitosan and 5 mL acetone were mixed ultrasonically for more than 30 min., around 50–75  $\mu\text{L}$  of this slurry was dropped onto the freshly polished GCE via a syringe. After the acetone evaporated completely, the prepared electrode ( $\text{Co}_3\text{O}_4\text{-BiPO}_4/\text{GCE}$ ) was used as the working electrode after drying in an oven.

## 2.4. XRD and TEM

The qualitative of  $\text{Co}_3\text{O}_4\text{-BiPO}_4$  nanocomposite was characterized using XRD and TEM. Various samples were identified by the  $2\theta$  angles, and the crystal parameters were

estimated by X-ray diffractometer (Shimadzu Scientific Instruments (SSI), Shimadzu Lab-X XRD-6000; X-ray tube: Cu  $K\alpha$  radiation (1.54060 Å), voltage: 40.0 keV and current: 30.0 mA). The XRD-6000 boasts an integrated design featuring high speed and a high precision vertical goniometer (compact design; 900 × 700 × 1600 mm ( $w \times d \times h$ , in mm) suitable for diverse applications and data processing software supporting the Windows XP user interface. The  $2\theta$  scanning range was between 10 and 80°, at a scan rate of 4°/min.

The morphology of the sensing materials was studied by high-resolution transmission electron microscope (JEOL 2010 TEM—accelerating voltage: 200 kV, analytical mode, LaB6 filament; vacuum system operates in the  $10^{-9}$  Torr range, max. tilt angle in goniometer was 25°; higher resolution imaging with 0.23 nm point resolution; single-tilting and double-tilting sample holders/stages and capable of Bright-Field, Dark-Field imaging, SAED and CBED electron diffraction) equipped with Gatan Erlangshen CCD camera (Gatan SC1000, 4008 × 2672 pixels image size—the CCD active area is 36 × 24 mm), high-definition video recording software and TSL texture analysis system.

## 2.5. Electrochemical Detection System

The electrochemical behaviour of  $\text{Co}_3\text{O}_4$ ,  $\text{BiPO}_4$  and  $\text{Co}_3\text{O}_4\text{-BiPO}_4$  have been carried out using cyclic voltammetry and differential pulse voltammetry (ZIVE SP1 compact type Electrochemical Workstation, WonATech Co., Ltd., Seocho-gu, Seoul, South Korea; <http://www.wonatech.com>). The Zive SP1 is a compact type  $\pm 1$  amp single channel electrochemical workstation having the capability of electrochemical impedance spectroscopy (EIS) with a single auxiliary voltage reading, can be used for multichannel operation with SIM4U is digital cyclic voltammogram simulation software (Ver. 2.1). In this electrochemical system, the three-electrodes were used; GCE was used as a working electrode, a saturated Ag/AgCl electrode as a reference electrode and platinum wire as a counter electrode, as shown in Figure 2.

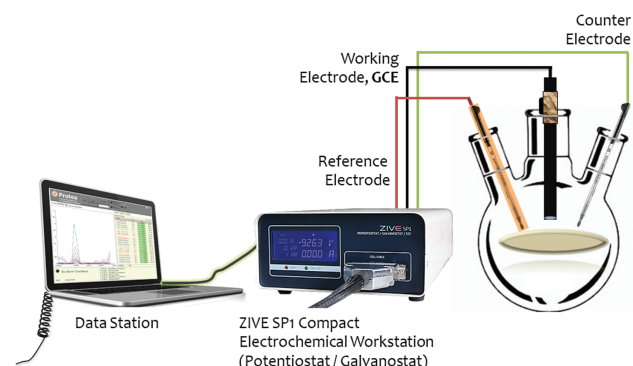


**Figure 2.** Setup for the electrochemical detection of epinephrine.

### 3. RESULTS AND DISCUSSION

#### 3.1. Characterization of the $\text{Co}_3\text{O}_4\text{-BiPO}_4$ Nanocomposite

XRD patterns were recorded by a Shimadzu Lab-X-6000 X-ray diffractometer using  $\text{Cu K}\alpha$  radiation. The XRD spectra of various samples (a)  $\text{BiPO}_4$  (b)  $\text{Co}_3\text{O}_4\text{-BiPO}_4$  (c)  $\text{Co}_3\text{O}_4$  are revealed in Figure 3. Different diffraction patterns were compared with the JPCDS database. All of the reflection peaks could be readily indexed to crystalline cubic phase  $\text{Co}_3\text{O}_4$  with a lattice constant of  $a = 8.065 \text{ \AA}$ , which is consistent with the standard value of  $a = 8.065 \text{ \AA}$  (JCPDS Card file No. 74-1656). Figure 3(a) the diffraction peaks of  $\text{BiPO}_4$  with main lattice plane are (101), (200), (102) and (211) compared with JCPDS, which are a similar hexagonal phase. According to characteristic peaks proved the successful synthesis of  $\text{Co}_3\text{O}_4\text{-BiPO}_4$  by hydrothermal methods shown in Figure 3(b) [15]. Figure 3(c) shows the intense diffraction peaks of  $\text{Co}_3\text{O}_4$  with lattice planes (111), (220), (311), (222), (400), (422), (511) and (440) separately. The mean crystallite sizes of  $\text{Co}_3\text{O}_4$  (311) were calculated using the Debye–Scherrer formula as 20.3 nm and 13.2 nm to  $\text{Co}_3\text{O}_4$  and  $\text{Co}_3\text{O}_4\text{-BiPO}_4$ , respectively. This means that a portion of  $\text{Co}_3\text{O}_4$  was effectively dispersed on  $\text{BiPO}_4$  and the particle size of  $\text{Co}_3\text{O}_4\text{-BiPO}_4$  was smaller than that of bulk  $\text{Co}_3\text{O}_4$ . The mean crystalline size of the  $\text{BiPO}_4$  (200) nanoparticles is estimated as 17.1 nm. The data is summarised in Table I.

Figures 4(i) to (vi) revealed that the TEM images of  $\text{Co}_3\text{O}_4$ ,  $\text{BiPO}_4$  and  $\text{Co}_3\text{O}_4\text{-BiPO}_4$ . TEM images of  $\text{Co}_3\text{O}_4$  at low magnification, scale 100 nm and at higher magnification, scale 10 nm were given in Figures 4(i) and (ii). It revealed some sphere like powders were distribution, and the diameter of the crystalline to  $\text{Co}_3\text{O}_4$  (311) was estimated as 13.4 nm. Figure 4(iii) shows a TEM image of single  $\text{BiPO}_4$  nanorod with 570 nm in length and 98 nm in width. Figure 4(iv) presents the TEM image

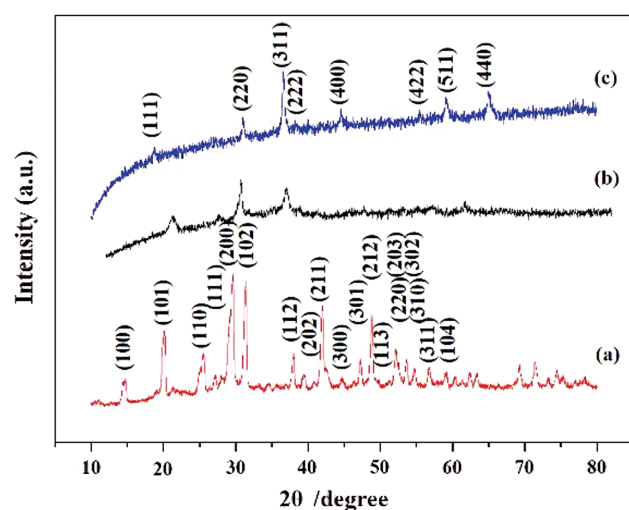


**Figure 3.** XRD patterns of various samples (a)  $\text{BiPO}_4$  (b)  $\text{Co}_3\text{O}_4\text{-BiPO}_4$  (c)  $\text{Co}_3\text{O}_4$ .

**Table I.** Crystalline grain size of various sensing materials by XRD and TEM.

Sensing materials	Crystalline grain size (nm)	
	XRD	TEM
$\text{Co}_3\text{O}_4$ (311)	20.3 nm	13.4 nm
$\text{BiPO}_4$ (200)	17.1 nm	11.0 nm
$\text{Co}_3\text{O}_4\text{-BiPO}_4$	13.2 nm	11.9 nm
	$\text{Co}_3\text{O}_4$ (311)	$\text{Co}_3\text{O}_4$ (311)

of  $\text{BiPO}_4$  (200) lattice plane which was about 0.33 nm lattice displace. A TEM image of  $\text{Co}_3\text{O}_4\text{-BiPO}_4$  at low magnification scale 200 nm is revealed in Figure 4(v), it appears some rod-like structure. Figure 4(vi) shows the TEM image of  $\text{BiPO}_4$  (200) lattice plane which was about  $d = 0.33 \text{ nm}$  and  $\text{Co}_3\text{O}_4$  (311) lattice displace  $d = 0.24 \text{ nm}$ .

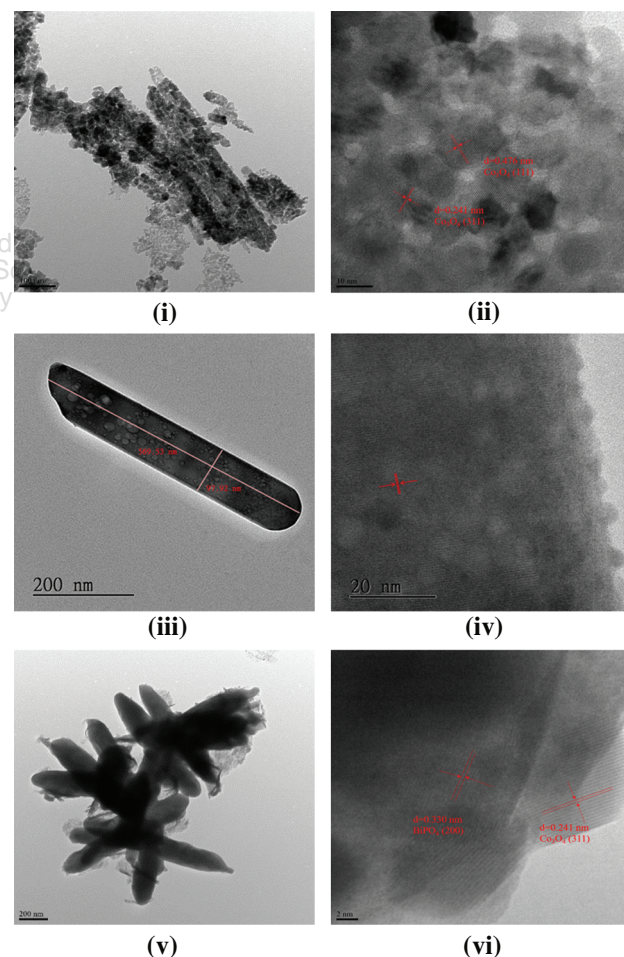


**Figure 4.** TEM images of  $\text{Co}_3\text{O}_4$  (i) image at low magnification, scale 100 nm, (ii) image at higher magnification, scale 10 nm; TEM images of  $\text{BiPO}_4$ , (iii) image at low magnification, scale 100 nm, (iv) image at higher magnification, scale 10 nm; TEM images of  $\text{Co}_3\text{O}_4\text{-BiPO}_4$ , (v) image at low magnification, scale 200 nm, (vi) image at higher magnification, scale 2 nm.

In Table I, the diameter of the Co<sub>3</sub>O<sub>4</sub> (311) particles (13.4 nm) was estimated using TEM, and it was similar to that estimated using the XRD data (20.3 nm). The diameter of the BiPO<sub>4</sub> nanoparticles is estimated as 11.0 nm, it is closed to the XRD calculation (17.1 nm). In Co<sub>3</sub>O<sub>4</sub>-BiPO<sub>4</sub>, the diameter of the Co<sub>3</sub>O<sub>4</sub> (311) particles (11.9 nm) is estimated using TEM, and it was similar to that estimated using the XRD data (13.2 nm).

### 3.2. Co<sub>3</sub>O<sub>4</sub>-BiPO<sub>4</sub> Electrochemical Behaviour

Experiments were carried out at a scan rate of 0.05 V · S<sup>-1</sup> with 0.9% NaCl, pH range 4.5–7.0, containing 55.00 μM of epinephrine. Figure 5(i) shows the cyclic voltammetry (CV) and Figure 5(ii) show differential pulse voltammetry (DPV) of GCE (a) bare (b) BiPO<sub>4</sub> and (c) Co<sub>3</sub>O<sub>4</sub>-BiPO<sub>4</sub> in NaCl and with 55.0 μM of EP. The measured current values are compared with three electrodes. It was revealed that the bare and BiPO<sub>4</sub> electrode had very little currents and the Co<sub>3</sub>O<sub>4</sub>-BiPO<sub>4</sub> modified electrode observed the oxidation peak had the high currents value at CV and DPV.

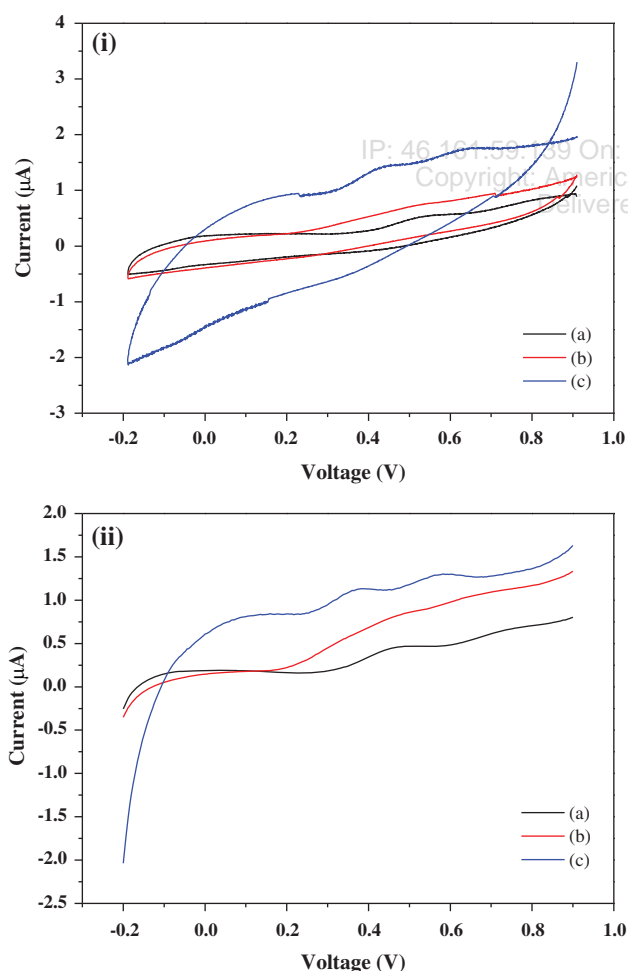


**Figure 5.** (i) CV response of (a) bare (b) BiPO<sub>4</sub> (c) Co<sub>3</sub>O<sub>4</sub>-BiPO<sub>4</sub> and (ii) DPV response of (a) bare (b) BiPO<sub>4</sub> (c) Co<sub>3</sub>O<sub>4</sub>-BiPO<sub>4</sub>.

With the change of concentration, epinephrine was determined using CV and DPV. The CV of Co<sub>3</sub>O<sub>4</sub>-BiPO<sub>4</sub> profiled two oxidation peak at 0.447 and 0.645 V in the concentration of EP from 1.72 μM to 55.0 μM at scan rate 50 mV · S<sup>-1</sup> in the potential range from -0.2~0.9 V. The linear calibration for oxidation peak current versus EP concentration is shown in Figure 6 with resultant linear equation of  $I_{pa} (\mu\text{M}) = 0.0192 (\mu\text{M}) + 21.90$  ( $R^2 = 0.9973$ ) at 0.645 V and  $I_{pa} (\mu\text{M}) = 0.0139 (\mu\text{M}) + 0.7024$  ( $R^2 = 0.9792$ ) at 0.447 V.

Cyclic voltammetry curve of Co<sub>3</sub>O<sub>4</sub>-BiPO<sub>4</sub> electrode by varying the concentration of epinephrine (a) 55.00 μM (b) 27.50 μM (c) 13.75 μM (d) 6.88 μM (e) 3.44 μM (f) 1.72 μM (g) blank were shown in Figure 6(i) and Cyclic voltammetry calibration curve of Co<sub>3</sub>O<sub>4</sub>-BiPO<sub>4</sub> electrode by varying the concentration of epinephrine (a) 55.00 μM (b) 27.50 μM (c) 13.75 μM (d) 6.88 μM (e) 3.44 μM (f) 1.72 μM were shown in Figure 6(ii). Differential pulse voltammetry curve of Co<sub>3</sub>O<sub>4</sub>-BiPO<sub>4</sub>

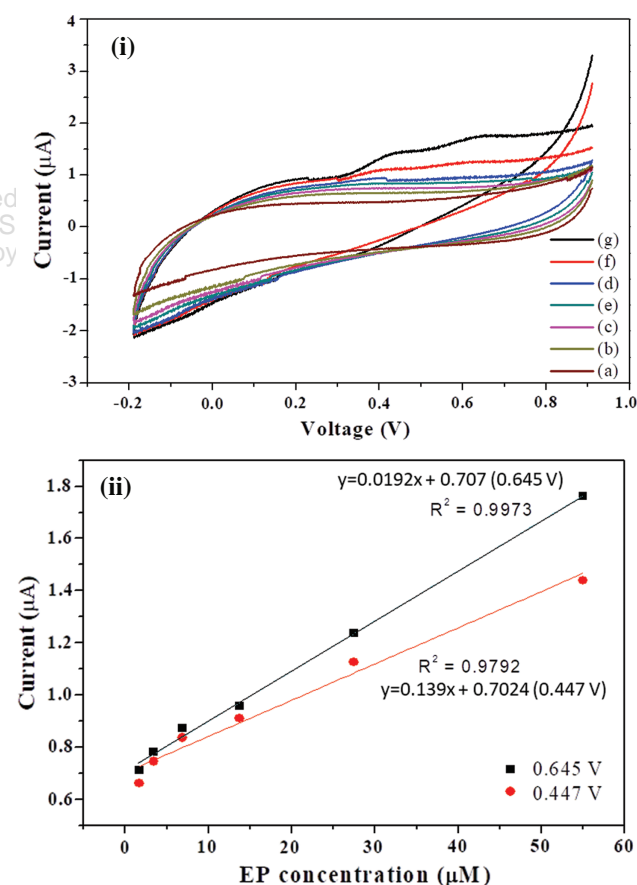


**Figure 6.** (i) Cyclic voltammetry curves of Co<sub>3</sub>O<sub>4</sub>-BiPO<sub>4</sub> electrode by varying the concentration of epinephrine (a) 55.00 μM (b) 27.50 μM (c) 13.75 μM (d) 6.88 μM (e) 3.44 μM (f) 1.72 μM (g) blank and (ii) cyclic voltammetry calibration curves of Co<sub>3</sub>O<sub>4</sub>-BiPO<sub>4</sub> electrode by varying the concentration of epinephrine (a) 55.00 μM (b) 27.50 μM (c) 13.75 μM (d) 6.88 μM (e) 3.44 μM (f) 1.72 μM.

electrode by varying the concentration of epinephrine (a) 55.00  $\mu\text{M}$  (b) 27.50  $\mu\text{M}$  (c) 13.75  $\mu\text{M}$  (d) 6.88  $\mu\text{M}$  (e) 3.44  $\mu\text{M}$  (f) 1.72  $\mu\text{M}$  (g) blank were given in Figure 7(i). Differential pulse voltammetry calibration curve of Co<sub>3</sub>O<sub>4</sub>-BiPO<sub>4</sub> electrode by varying the concentration of epinephrine (a) 55.00  $\mu\text{M}$  (b) 27.50  $\mu\text{M}$  (c) 13.75  $\mu\text{M}$  (d) 6.88  $\mu\text{M}$  (e) 3.44  $\mu\text{M}$  (f) 1.72  $\mu\text{M}$  were given in Figure 7(ii).

Using the DPV method with a scan rate of  $0.001 \text{ V} \cdot \text{S}^{-1}$ ,  $I_{\text{Range}} = 100 \mu\text{A}$ , the epinephrine oxidation peak was obtained at 0.384 V and 0.592 V with a good linear response in EP concentration vary. Linear equation of  $I_{\text{pa}} (\mu\text{M}) = 0.011 (\mu\text{M}) + 0.5662$  ( $R^2 = 0.9573$ ) at 0.384 V and  $I_{\text{pa}} (\mu\text{M}) = 0.0145 (\mu\text{M}) + 0.5348$  ( $R^2 = 0.9849$ ) at 0.592 V.

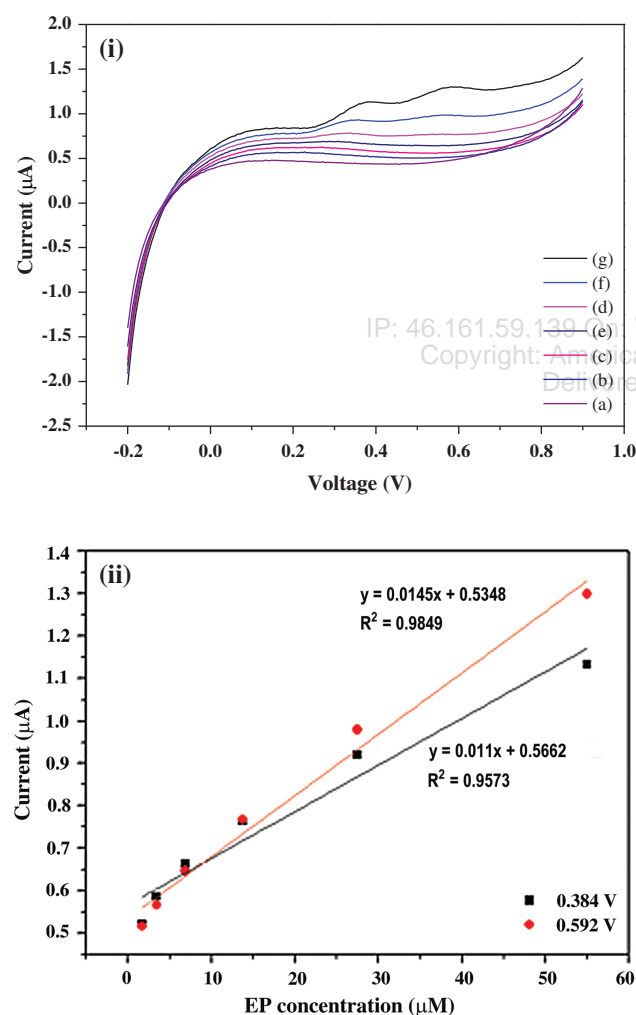


**Figure 7.** (i) Differential pulse voltammetry curve of Co<sub>3</sub>O<sub>4</sub>-BiPO<sub>4</sub> electrode by varying the concentration of epinephrine (a) 55.00  $\mu\text{M}$  (b) 27.50  $\mu\text{M}$  (c) 13.75  $\mu\text{M}$  (d) 6.88  $\mu\text{M}$  (e) 3.44  $\mu\text{M}$  (f) 1.72  $\mu\text{M}$  (g) blank and (ii) differential pulse voltammetry calibration curve of Co<sub>3</sub>O<sub>4</sub>-BiPO<sub>4</sub> electrode by varying the concentration of epinephrine (a) 55.00  $\mu\text{M}$  (b) 27.50  $\mu\text{M}$  (c) 13.75  $\mu\text{M}$  (d) 6.88  $\mu\text{M}$  (e) 3.44  $\mu\text{M}$  (f) 1.72  $\mu\text{M}$ .

### 3.3. Interference Test

In order to study the selectivity of Co<sub>3</sub>O<sub>4</sub>-BiPO<sub>4</sub> electrode, the effect of epinephrine with and without lidocaine in NaCl using the Chronoamperometry method was studied (see Fig. 8). Solutions containing both lidocaine and epinephrine were prepared and stored for usage. The influence of biological and pharmaceutical interferences on the epinephrine oxidation signal was studied in the presence of lidocaine. The obtained data confirmed the Co<sub>3</sub>O<sub>4</sub>-BiPO<sub>4</sub> has good selectivity for the determination of epinephrine. The sensor response obtained displayed higher sensor responses (%) of Co<sub>3</sub>O<sub>4</sub>-BiPO<sub>4</sub> for selective determination epinephrine; lidocaine was 11.6% less than the signal response compared with epinephrine. Chronoamperometry response for interference study for lidocaine and epinephrine is shown in Figure 8(i) and signal response obtained for lidocaine and epinephrine from chronoamperograms was is shown in Figure 8(ii).

### 3.4. Sensing Mechanism

The proposed mechanism is the electrocatalytic oxidation of epinephrine in Figure 9. The EP electro-oxidation pathway was debated many times in the literature [16], but in fact, it was neither totally clear nor properly established. In this study, we propose EP electrocatalytic oxidation mechanism initiated by the electron transfer between Co<sub>3</sub>O<sub>4</sub> and epinephrine followed by catalytic oxidation through BiPO<sub>4</sub> which is within the nanocomposite

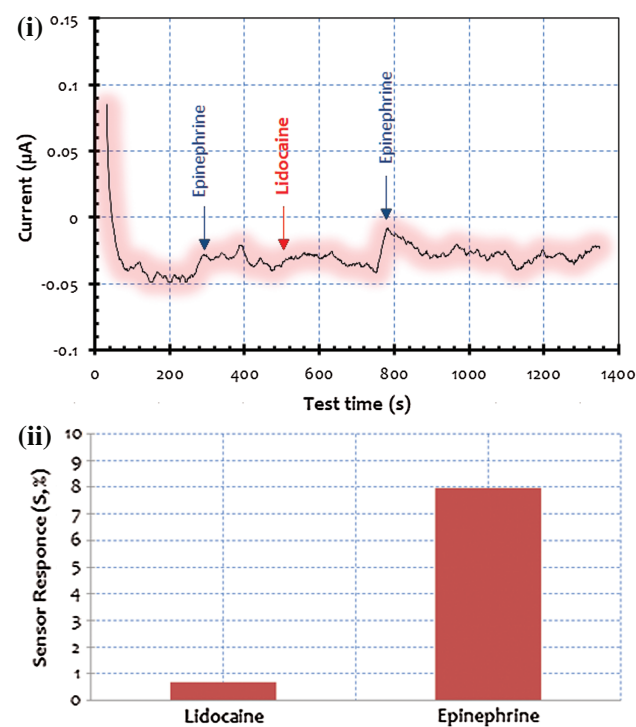


**Figure 8.** (i) Chronoamperometry response for interference study for lidocaine and epinephrine and (ii) signal response obtained for lidocaine and epinephrine from chronoamperograms.

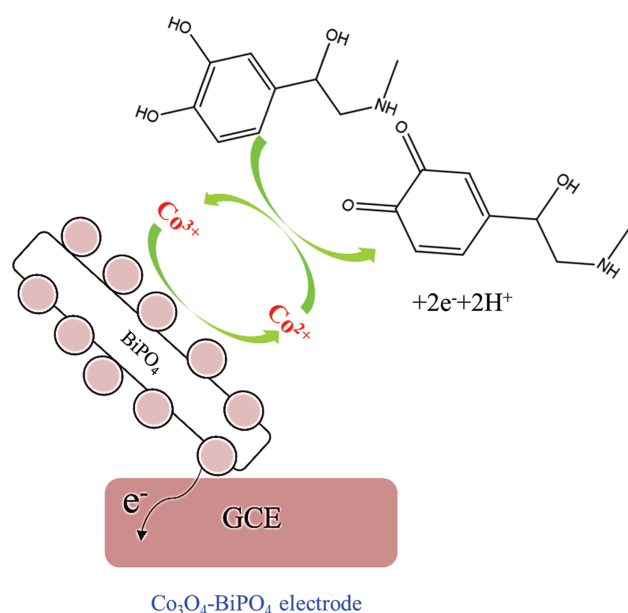


**Figure 9.**  $\text{Co}_3\text{O}_4\text{-BiPO}_4$  electrocatalytic oxidation mechanism for determining epinephrine.

makes it possible for quicker electrochemical detection of epinephrine at the GCE electrode which seems more feasible. Comparing to the data in Table I, the diameter of the  $\text{Co}_3\text{O}_4$  (311) particle in  $\text{Co}_3\text{O}_4\text{-BiPO}_4$  sample is smaller than  $\text{Co}_3\text{O}_4$ . It is to say the  $\text{Co}_3\text{O}_4$  sample was dispersion on  $\text{BiPO}_4$  of  $\text{Co}_3\text{O}_4\text{-BiPO}_4$  sensing material. Figure 9 reveals the role of  $\text{Co}_3\text{O}_4$  is a catalytic chemical oxidation reaction centre and it happens reversibly in two cobalt metal ions  $\text{Co}^{+2}$  and  $\text{Co}^{+3}$  metal oxides [10, 11]. According to the data of Table I, the  $\text{Co}_3\text{O}_4$  sample was dispersion on  $\text{BiPO}_4$  of  $\text{Co}_3\text{O}_4\text{-BiPO}_4$  sensing material. So the active centre on  $\text{Co}_3\text{O}_4$  particle of  $\text{Co}_3\text{O}_4\text{-BiPO}_4$  sensing material is increased than the bulk  $\text{Co}_3\text{O}_4$ . And the role of  $\text{BiPO}_4$  is only a supporting material, for the currents of  $\text{BiPO}_4$  electrode are very little in Figures 5(i) and (ii).

#### 4. CONCLUSION

In this work, electrochemical sensor fabricated from hydrothermally synthesized  $\text{Co}_3\text{O}_4\text{-BiPO}_4$  material was investigated for epinephrine detection, which can play a significant role as an electrochemical sensor for detection of epinephrine.  $\text{Co}_3\text{O}_4\text{-BiPO}_4$  nanocomposite was synthesized and incorporated onto the surface of a carbon paste electrode as a highly sensitive sensor for epinephrine analysis. Sensing material  $\text{Co}_3\text{O}_4\text{-BiPO}_4$  system was characterized using X-ray diffraction (XRD), transmission electron microscope (TEM) techniques. The  $\text{Co}_3\text{O}_4\text{-BiPO}_4$  system was used as a glassy carbon electrode material in detecting epinephrine. Based on the experimental results, it revealed that the epinephrine concentration range of 1.71–55.00  $\mu\text{M}$  has a very wide linear response with CV and DPV. However, the  $\text{Co}_3\text{O}_4\text{-BiPO}_4$  electrode used

in Chronoamperometry method showed the highest selectivity and lowest detection limit ( $\text{LOD} = 1.334 \mu\text{M}$ ) at 0.645 V. The CV and DPV method of electrochemistry for epinephrine detection has certain advantages of ease of operation, low cost and rapid analysis. Finally, the  $\text{Co}_3\text{O}_4\text{-BiPO}_4$  was used for the analysis of epinephrine in real samples. From these studies, the good linear relationship can be used for the determination of EP in practical purposes, with fast and precise results. An electrocatalytic oxidation mechanism for epinephrine detection was proposed using the  $\text{Co}_3\text{O}_4\text{-BiPO}_4$  electrode. Also from the results, the work can be extended on  $\text{BiPO}_4$  photocatalyst by focusing on the design and synthesis of more effective nanostructures.

**Acknowledgments:** This work was supported by the Ministry of Science and Technology (MOST) in Taiwan under the grant number MOST 107-2113-M-126-003.

#### References and Notes

- Zhang, G., Zhang, Y., Ji, C., McDonald, T., Walton, J., Groeber, E.A., Steenwyk, R.C. and Lin, Z., **2012**. Ultra-sensitive measurement of endogenous epinephrine and norepinephrine in human plasma by semi-automated SPE-LC-MS/MS. *Journal of Chromatography B*, 895(5), pp.186–190.
- Davletbaeva, P., Falkova, M., Safonova, E., Moskvin, L. and Bulatov, A., **2016**. Flow method based on cloud point extraction for the fluorometric determination of epinephrine in human urine. *Analytica Chimica Acta*, 911(10), pp.69–74.
- Li, T., Wang, Z., Xie, H. and Fu, Z., **2012**. Highly sensitive trivalent copper chelate-luminol chemiluminescence system for capillary electrophoresis detection of epinephrine in the urine of smoker. *Journal of Chromatography B*, 911(6), pp.1–5.
- Wierzbička, E. and Sulka, G.D., **2016**. Nanoporous sponge like Au–Ag films for electrochemical epinephrine sensing. *Journal of Electroanalytical Chemistry*, 762(1), pp.43–50.
- Wierzbička, E., Małgorzata S.M., Buszewski, B., Grzegorz, D. and Sulka, G.D., **2016**. Epinephrine sensing at nanostructured Au electrode and determination its oxidative metabolism. *Sensors and Actuators B*, 237(12), pp.206–215.
- Li, Y., Ali, M.M.A., Chen, S.M., Yang, S.Y., Lou, B.S. and Al-Hemaid, F.M.A., **2014**. Poly(basic red 9) doped functionalized multi-walled carbon nanotubes as composite films for neurotransmitters biosensors. *Colloids and Surfaces B: Biointerfaces*, 118(6), pp.133–139.
- Ozoemena, K.I., Nkosi, D. and Pillay, J., **2008**. Influence of solution pH on the electron transport of the self-assembled nanoarrays of single-walled carbon nanotube-cobalt tetra-amino-phthalocyanine on gold electrodes, Electrocatalytic detection of epinephrine. *Electrochimica Acta*, 53(6), pp.2844–2851.
- Ariga, K., Ji, Q., Nakanishi, W., Hill, J.P. and Aono, M., **2015**. Nanoarchitectonics: A new materials horizon for nanotechnology. *Materials Horizons*, 2(4), pp.406–413.
- Ariga, K., Minami, K., Ebara, M. and Nakanishi, J., **2016**. What are the emerging concepts and challenges in NANO? Nanoarchitectonics, hand-operating nanotechnology and mechanobiology. *Polymer Journal*, 48(4), pp.371–389.
- Zhang, Q., Mo, S., Chen, B., Zhang, W., Huang, C. and Ye, D., **2018**. Hierarchical  $\text{Co}_3\text{O}_4$  nanostructures *in-situ* grown on 3D nickel foam towards toluene oxidation. *Molecular Catalysis*, 454(7), pp.12–20.

11. Li, A., Wang, C., Zhang, H., Zhao, Z.Z., Wang, J., Cheng, M., Zhao, H., Wang, J., Wu, M. and Wang, J., **2018**. Graphene-supported atomic Co/nanocrystalline Co<sub>3</sub>O<sub>4</sub> for oxygen evolution reaction. *Electrochimica Acta*, 276(6), pp.153–161.
12. Ando, M., Kobayashi, T., Iijima, S. and Haruta, H., **1997**. Optical recognition of CO and H<sub>2</sub> by use of gas-sensitive Au-Co<sub>3</sub>O<sub>4</sub> composite films. *Journal of Material Chemistry*, 7(9), pp.1779–1783.
13. She, L., Tan, G., Ren, H., Huang, J., Xu, C. and Ao Xia, A., **2015**. Photocatalytic and photoelectrochemical activity of N-doped BiPO<sub>4</sub> photocatalyst. *RSC Advanced*, 5(46), pp.36642–36651.
14. Wang, X., Chen, X., Gao, L., Zheng, H., Zhang, Z. and Qian, Y., **2004**. One-dimensional arrays of Co<sub>3</sub>O<sub>4</sub> nanoparticles: Synthesis, characterization, and optical and electrochemical properties. *Journal of Physical Chemistry B*, 108(42), pp.16401–16404.
15. Wu, R.J., Wu, J.G., Tsai, T.G. and Yeh, Y.T., **2006**. Use of cobalt oxide CoOOH in a carbon monoxide sensor operating at low temperatures. *Sensors and Actuators B*, 120(1), pp.104–109.
16. Kim, S.H., Lee, J.W. and Yeo, I.H., **2000**. Spectroelectrochemical and electrochemical behaviour of epinephrine at a gold electrode. *Electrochimica Acta*, 45(18), pp.2889–2895.

Received: 15 March 2019. Accepted: 9 June 2019.

IP: 46.161.59.139 On: Wed, 01 Jan 2020 14:17:56  
Copyright: American Scientific Publishers  
Delivered by Ingenta